Bulgarian Chemical Communications, Volume 46, Number 3 (pp. 545 – 555) 2014

Systematic parameter study for nano-fiber fabrication *via* electrospinning process

M. Mohammadian[1], A. K. Haghi[2*]

[1]*Department of Textile Engineering, Kashan Branch, Islamic Azad University, Kashan, Iran*
[2]*University of Guilan, P.O.Box 3756, Rasht, Iran*

Received July 16, 2013; Revised August 29, 2013

Elecrospinning is a process that produces continuous polymer fibers with diameter in the submicron range. In the electrospinnig process the electric body force acts on the elements of a charged fluid. Electrospinning has emerged as a specialized processing technique for the formation of sub-micron fibers (typically between 100 nm and 1 μm in diameter), with high specific surface area. The objective of this paper is to establish quantitative relationships between the electrospinning parameters and the mean and standard deviation of fiber diameter, as well as to evaluate the effectiveness of the empirical models with a set of test data.

Keywords: Electrospinning, Nanofibers, Fiber diameter, Processing variables, Response surface methodology

INTRODUCTION

Electrospinning is a novel and efficient method to produce fibers with diameters in the nanometer scale, named nanofibers. In the electrospinning process, a strong electric field is applied on a droplet of polymer solution (or melt) held by its surface tension at the tip of a syringe needle (or a capillary tube) [1-5]. Fig. **1** shows a schematic illustration of an electrospinning setup.

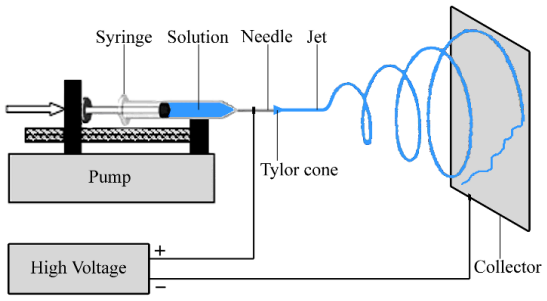

Fig. 1: Electrospinning setup [6]

Featuring various outstanding properties such as very small fiber diameters, large surface area per mass ratio [3], high porosity along with small pore sizes [7], flexibility, and superior mechanical properties [8], electrospun nanofiber mats have found numerous applications in biomedicine (tissue engineering [9]-[11], drug delivery [12], [13], wound dressing [14], [15]), protective clothing [7], filtration [16], reinforcement of composite mats [8], [17], micro-electronics (batteries [18], supercapacitors [19], transistors [20], sensors [21], and display devices [22-24]).

Among the characteristics of the final product such as physical, mechanical and electrical properties, fiber diameter is one of the most important structural features of electrospun nanofiber mats. Podgorski *et al*. [25] indicated that filters made of fibers with smaller diameters have higher filtration efficiency. This was also proved by the work of Qin *et al.* [16]. Ding *et al*. [26] reported that the sensitivity of sensors increases with decreasing the mean fiber diameter due to the higher surface area. In the study on designing polymer batteries consisting of electrospun PVdF fibrous electrolyte by Kim *et al.* [27], it was demonstrated that smaller fiber diameter results in a higher electrolyte uptake and thereby increased ionic conductivity of the mat. Moroni *et al.* [28] found that fiber diameters of electrospun PEOT/PBT scaffolds influence cell seeding, attachment and proliferation. The carbonization and activation conditions, as well as the structure and properties of the ultimate carbon fibers are also affected by the diameters of the precursor PAN nanofibers [29]. Consequently, precise control of the electrospun fiber diameter is very crucial.

Sukigara *et al.* [30] employed response surface methodology (RSM) to model mean fiber diameter of electrospun regenerated Bombyx mori silk with electric field and concentration at two spinning distances.

Gu *et al.* [31] and Gu *et al.* [32] also exploited the RSM for quantitative study of PAN and PDLA.

* To whom all correspondence should be sent:
E-mail: Haghi@Guilan.ac.ir

In the most recent investigation in this field, Yördem *et al.* [33] utilized RSM to correlate the mean and coefficient of variation (CV) of the diameter of electrospun PAN nanofibers to solution concentration and applied voltage at three different spinning distances.

Several patents are reported on the process for production of ultrahigh-tensile strength PVA fibers comparable to Kevlar® [36]-[38]. PVA has found many applications in biomedical uses as well, due to its biocompatibility [39]. For instance, PVA hydrogels were used in regenerating articular cartilages [40], [41], artificial pancreas [42], and drug delivery systems [43], [44]. More recently, PVA nanofibers were electrospun and used as a protein delivery system [45], for retardation of enzyme release [45] and wound dressing [46].

In this paper, response surface methodology (RSM) was employed to quantitatively investigate the simultaneous effects of four of the most important parameters, namely solution concentration (*C*), spinning distance (*d*), applied voltage (*V*) and volume flow rate (*Q*) on the mean fiber diameter (MFD) and the standard deviation of the fiber diameter (StdFD) in electrospinning of polyvinyl alcohol (PVA) nanofibers.

EXPERIMENTAL

Solution preparation and electrospinning

PVA with molecular weight of 72000 g/mol and degree of hydrolysis of >98% was obtained from Merck and was used as received. Distilled water was added as a solvent to a predetermined amount of PVA powder to obtain 20 ml of a solution with desired concentration. The solution was prepared at 80°C and was gently stirred for 30 min to expedite the dissolution. After the PVA had completely dissolved, the solution was transferred to a 5 ml syringe and was ready to electrospin. The experiments were carried out on a horizontal electrospinning setup shown schematically in **Fig. 1**. The syringe containing PVA solution was placed on a syringe pump (New Era NE-100) used to dispense the solution at a controlled rate. A high voltage DC power supply (Gamma High Voltage ES-30) was used to generate the electric field needed for electrospinning. The positive electrode of the high voltage supply was attached to the syringe needle via an alligator clip and the grounding electrode was connected to a flat collector wrapped with aluminum foil where electrospun nanofibers were accumulated to form a nonwoven mat. The electrospinning was carried out at room temperature. Subsequently, the aluminum foil was removed from the collector. A small piece of mat was placed on the sample holder and gold sputter-coated (Bal-Tec). Thereafter, the morphology of the electrospun PVA fibers was observed by an environmental scanning electron microscope (SEM, Phillips XL-30) under magnification of 10000×. For each specimen, fiber diameter distribution was determined from the SEM micrograph based on 100 measurements of random fibers. A typical SEM micrograph of an electrospun nanofiber mat and its corresponding diameter distribution are shown in Fig. ***2***.

Choice of parameters and range

In this study, solution concentration (*C*), spinning distance (*d*), applied voltage (*V*), and volume flow rate (*Q*) were selected to be the most influential parameters in electrospinning of PVA nanofibers for the purpose of this study.

The relationship between intrinsic viscosity ($[\eta]$) and molecular weight (*M*) is given by the well-known Mark-Houwink-Sakurada equation as follows:

$$[\eta] = KM^{a} \quad (1)$$

where *K* and *a* are constants for a particular polymer-solvent pair at a given temperature [47]. For the PVA with molecular weight in the range of 69000 *g*/*mol* <*M*<690000 *g*/*mol* in water at room

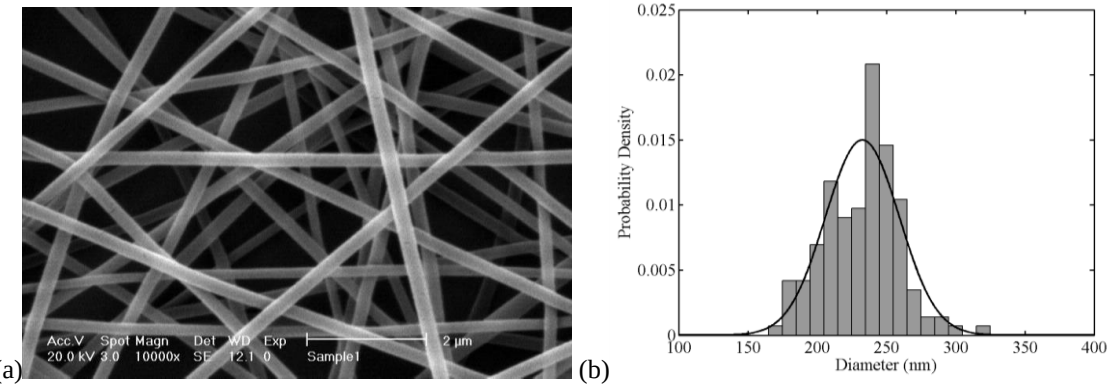

Fig. 2. (a) a typical SEM micrograph of electrospun nanofiber mat, (b) its corresponding diameter distribution

temperature, K=6.51 and a=0.628 were found by Tacx *et al*. [48]. Using these constants in the equation, the intrinsic viscosity of PVA in this study (molecular weight of 72000 *g*/*mol*) were calculated to be $[\eta]$=0.73.

Polymer chain entanglements in a solution can be expressed in terms of Berry number (B), which is a dimensionless parameter and is defined as the product of intrinsic viscosity and polymer concentration ($B=[\eta]C$) [49]. At each molecular weight, there is a minimum concentration at which the polymer solution cannot be electrospun. Koski *et al.* [50] observed that B>5 is required to form stabilized fibrous structures in electrospinning of PVA. On the other hand, they reported the formation of flat fibers at B>9. Therefore, the appropriate range in this case could be found within the 5<B<9 domain which is equivalent to 6.8%<C<12.3% in terms of concentration of PVA. Furthermore, Koski *et al*. [50] observed that beaded fibers were electrospun at low solution concentration. Hence, it was thought that the domain 8%≤C≤12% would warrant the formation of stabilized bead-free fibers with circular cross-sections. This domain was later justified by some preliminary experiments.

For determining the appropriate range of applied voltage, referring to previous works, it was observed that the changes of voltage lay between 5 *kV* and 25 *kV* depending on experimental conditions; voltages above 25 *kV* were rarely used. Afterwards, a series of experiments was carried out to obtain the desired voltage domain. At V<10 *kV*, the voltage was too low to spin fibers and 10 *kV*≤V<15 *kV* resulted in formation of fibers and droplets; in addition, electrospinning was impeded at high concentrations. In this regard, 15 *kV*≤V≤25 *kV* was selected as the desired domain for the applied voltage.

The use of 5 *cm* – 20 *cm* for spinning distance was reported in the literature. Short distances are suitable for highly evaporative solvents whereas wet conglutinated fibers are obtained with nonvolatile solvents due to insufficient evaporation time. Since water was used as a solvent for PVA in this study, short spinning distances were not expected to be favorable for dry fiber formation. Afterwards, this was proved by experimental observations and 10 *cm*≤d≤20 *cm* was considered as the effective range for the spinning distance.

Few researchers have addressed the effect of volume flow rate. Therefore, in this case, the attention was focused on experimental observations. At Q<0.2 *ml*/*h*, in most cases, especially at high polymer concentrations, fiber formation was hindered due to insufficient supply of solution to the tip of the syringe needle, whereas excessive feed of solution at Q>0.4 *ml*/*h* incurred formation of droplets along with fibers. As a result, 0.2 *ml*/*h*≤Q≤0.4 *ml*/*h* was chosen as the favorable range of flow rate in this study.

Experimental design

Three levels were selected for each parameter in this study so that it would be possible to use quadratic models. These levels were chosen equally spaced. A full factorial experimental design with four factors (solution concentration, spinning distance, applied voltage, and flow rate) each at three levels (3^4 design) was employed, resulting in 81 treatment combinations. This design is shown in Fig. **3**.

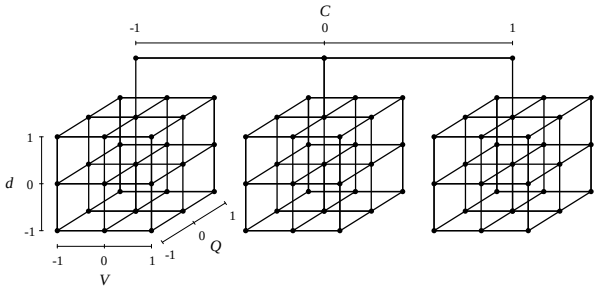

Fig. 3. 3^4 Full factorial experimental design used in this study

-1, 0, and 1 are coded variables corresponding to low, intermediate and high levels of each factor respectively. The coded variables (x_j) were calculated using Equation (2) from natural variables (ξ_i). The indices 1 to 4 represent solution concentration, spinning distance, applied voltage, and flow rate, respectively. In addition to the experimental data, 15 treatments inside the design space were selected as test data and were used for evaluation of the models. The natural and coded variables for experimental data (numbers 1-81) as well as test data (numbers 82-96) are listed in listed in Table 6.

$$x_j = \frac{\xi_j - [\xi_{hj} + \xi_{lj}]/2}{[\xi_{hj} - \xi_{lj}]/2} \tag{2}$$

Response surface methodology

The relationship between the response (y) and k input variables ($\xi_1,\xi_2,...,\xi_k$) could be expressed in terms of mathematical notations as follows:

$$y = f(\xi_1, \xi_2, ..., \xi_k) \tag{3}$$

where the true response function f is unknown. It is often convenient to use coded variables ($x_1,x_2,..,x_k$) instead of natural (input) variables. The response function will then be:

$$y = f(x_1, x_2, ..., x_k) \tag{4}$$

Since the form of true response function *f* is unknown, it must be approximated. Therefore, the successful use of RSM is critically dependent upon the choice of appropriate function to approximate *f*. Low-order polynomials are widely used as approximating functions. First-order (linear) models are unable to capture the interaction between parameters which is a form of curvature in the true response function. A second-order (quadratic) model will likely perform well in these circumstances. In general, the quadratic model is in the form of:

$$y = \beta_0 + \sum_{j=1}^{k} \beta_j x_j + \sum_{j=1}^{k} \beta_{jj} x_j^2 + \sum_{i<j} \sum_{j=2}^{k} \beta_{ij} x_i x_j + \varepsilon \qquad (5)$$

where ε is the error term in the model. The use of polynomials of higher order is also possible but infrequent. The βs are a set of unknown coefficients needed to be estimated. In order to do that, the first step is to make some observations on the system being studied. The model in Equation (5) may now be written in matrix notations as:

$$\mathbf{y} = \mathbf{X}\boldsymbol{\beta} + \boldsymbol{\varepsilon} \qquad (6)$$

where $\mathbf{y}$ is the vector of observations, $\mathbf{X}$ is the matrix of levels of the variables, $\boldsymbol{\beta}$ is the vector of unknown coefficients, and $\boldsymbol{\varepsilon}$ is the vector of random errors. Afterwards, the method of least squares, which minimizes the sum of squares of errors, is employed to find the estimators of the coefficients ($\hat{\boldsymbol{\beta}}$) through:

$$\hat{\boldsymbol{\beta}} = (\mathbf{X}'\mathbf{X})^{-1}\mathbf{X}'\mathbf{y} \qquad (7)$$

The fitted model will then be written as:

$$\hat{\mathbf{y}} = \mathbf{X}\hat{\boldsymbol{\beta}} \qquad (8)$$

Finally, response surfaces or contour plots are depicted to help visualize the relationship between the response and the variables and see the influence of the parameters [53].

RESULTS AND DISCUSSION

After the unknown coefficients (βs) were estimated by the least squares method, the quadratic models for the mean fiber diameter (MFD) and standard deviation of fiber diameter (StdFD) in terms of coded variables are written as:

$$\begin{aligned} \text{MFD} = {} & 282.031 + 34.953 x_1 + 5.622 x_2 - 2.113 x_3 + 9.013 x_4 \\ & - 11.613 x_1^2 - 4.304 x_2^2 - 15.500 x_3^2 \\ & - 0.414 x_4^2 + 12.517 x_1 x_2 + 4.020 x_1 x_3 \\ & - 0.162 x_1 x_4 + 20.643 x_2 x_3 + 0.741 x_2 x_4 + 0.877 x_3 x_4 \end{aligned} \qquad (9)$$

$$\begin{aligned} \text{MFD} = {} & 282.031 + 34.953 x_1 + 5.622 x_2 - 2.113 x_3 + 9.013 x_4 \\ & - 11.613 x_1^2 - 4.304 x_2^2 - 15.500 x_3^2 \\ & - 0.414 x_4^2 + 12.517 x_1 x_2 + 4.020 x_1 x_3 \\ & - 0.162 x_1 x_4 + 20.643 x_2 x_3 + 0.741 x_2 x_4 + 0.877 x_3 x_4 \end{aligned} \qquad (10)$$

In the next step, a couple of very important hypothesis-testing procedures were carried out to measure the usefulness of the models presented here. First, the test for significance of the model was performed to determine whether there is a subset of variables which contributes significantly in representing the response variations. The appropriate hypotheses are:

$$\begin{aligned} & H_0 : \beta_1 = \beta_2 = \cdots = \beta_k \\ & H_1 : \beta_j \neq 0 \quad \text{for at least one } j \end{aligned} \qquad (9)$$

The *p*-values of the models are very small (almost zero), therefore it is concluded that the null hypothesis is rejected in both cases suggesting that there are some significant terms in each model. There are also included in Table **1**, the values of R^2, R^2_{adj}, and R^2_{pred}. R^2 is a measure of the amount of response variation which is explained by the variables and will always increase when a new term is added to the model – regardless of whether the inclusion of the additional term is statistically significant or not. R^2_{adj} is the R^2 adjusted for the number of terms in the model, therefore it will increase only if the new terms improve the model and decreases if unnecessary terms are added. R^2_{pred} implies how well the model predicts the response for new observations, whereas R^2 and R^2_{adj} indicate how well the model fits the experimental data. The R^2 values demonstrate that 95.74% of MFD and 89.92% of StdFD are explained by the variables. The R^2_{adj} values are 94.84% and 87.78% for MFD and StdFD respectively, which account for the number of terms in the models. Both R^2 and R^2_{adj} values indicate that the models fit the data very well. The slight difference between the values of R^2 and R^2_{adj} suggests that there might be some insignificant terms in the models. Since the R^2_{pred} values are so close to the values of R^2 and R^2_{adj}, the models does not appear to be overfit and have very good predictive ability.

The second testing hypothesis performed in this study was the test on individual coefficients, which would be useful in determining the value of the variables in the models. The hypotheses for testing the significance of any individual coefficient are:

$$\begin{aligned} & H_0 : \beta_j = 0 \\ & H_1 : \beta_j \neq 0 \end{aligned} \qquad (10)$$

Table 1. Summary of the results from the statistical analysis of the models

	F	p-value	R^2	R^2_{adj}	R^2_{pred}
MFD	106.02	0.000	95.74%	94.84%	93.48%
StdFD	42.05	0.000	89.92%	87.78%	84.83%

Since the model might be more effective with inclusion or perhaps exclusion of one or more variables, by means of this test, we could evaluate the value of each term in the model and eliminate the statistically insignificant terms, thereby obtain more efficient models. The results of this test for the models of MFD and StdFD are summarized in Table 2 and Table 3, respectively.

Table 2. Test on individual coefficients for the model of mean fiber diameter

Term	Coef.	T	p-value
Constant	282.031	102.565	0.000
C	34.953	31.136	0.000
d	5.622	5.008	0.000
V	-2.113	-1.882	0.064
Q	9.013	8.028	0.000
C^2	-11.613	-5.973	0.000
d^2	-4.304	-2.214	0.030
V^2	-15.500	-7.972	0.000
Q^2	-0.414	-0.213	0.832
Cd	12.517	9.104	0.000
CV	4.020	2.924	0.005
CQ	-0.162	-0.118	0.906
dV	20.643	15.015	0.000
dQ	0.741	0.539	0.592
VQ	0.877	0.638	0.526

Table 3: Test on individual coefficients for the model of standard deviation of fiber diameter

Term	Coef.	T	p-value
Constant	36.1574	39.381	0.000
C	4.5788	12.216	0.000
D	-1.5536	-4.145	0.000
V	6.4012	17.078	0.000
Q	1.1531	3.076	0.003
C^2	-2.2937	-3.533	0.001
d^2	-0.1115	-0.172	0.864
V^2	-1.1891	-1.832	0.072
Q^2	3.0980	4.772	0.000
Cd	-0.2088	-0.455	0.651
CV	1.0010	2.180	0.033
CQ	2.7978	6.095	0.000
dV	0.1649	0.359	0.721
dQ	-2.4876	-5.419	0.000
VQ	1.5182	3.307	0.002

As depicted, the terms Q^2, CQ, dQ, and VQ in the model of MFD and d^2, Cd, and dV in the model of StdFD have very high p-values, therefore they do not contribute significantly in representing the variation of the corresponding response. Eliminating these terms will enhance the efficiency of the models. Recalculating the unknown coefficients, the new models are then given by:

$$MFD = 281.755 + 34.953x_1 + 5.622x_2 - 2.113x_3 + 9.013x_4 - 11.613x_1^2 - 4.304x_2^2 - 15.500x_3^2 + 12.517x_1x_2 + 4.020x_1x_3 + 20.643x_2x_3 \quad (13)$$

$$StdFD = 36.083 + 4.579x_1 - 1.554x_2 + 6.401x_3 + 1.153x_4 - 2.294x_1^2 - 1.189x_3^2 + 3.098x_4^2 + 1.001x_1x_3 + 2.798x_1x_4 - 2.488x_2x_4 + 1.518x_3x_4 \quad (14)$$

in terms of coded variables and:

$$MFD = 10.3345 + 48.7288\,C - 22.7420\,d + 7.9713\,V + 90.1250\,Q - 2.9033\,C^2 - 0.1722\,d^2 - 0.6120\,V^2 + 1.2517\,Cd + 0.4020\,CV + 0.8257\,dV \quad (15)$$

$$StdFD = -1.8823 + 7.5590\,C + 1.1818\,d + 1.2709\,V - 300.3410\,Q - 0.5734\,C^2 - 0.0476\,V^2 + 309.7999\,Q^2 + 0.1001\,CV + 13.9892\,CQ - 4.9752\,dQ + 3.0364\,VQ \quad (16)$$

in terms of natural (uncoded) variables. The results of test for significance as well as R^2, R^2_{adj}, and R^2_{pred} for the new models are given in

Now that the relationships have been developed, the test data were used to investigate the prediction ability of the models. Root mean square errors (RMSE) between calculated responses (Ci)

Table 4. It is obvious that the p-values for the new models are close to zero indicating the existence of some significant terms in each model. Comparing the results of this table with Table **1**, the F statistic increased for the new models, indicating the improvement of the models after eliminating the insignificant terms. Despite the slight decrease in R^2, the values of R^2_{adj} and R^2_{pred} increased a great deal for the new models. The new models have the ability to better explain the experimental data. Due to higher R^2_{pred} values obtained, the new models also have higher prediction ability. In other words, eliminating the insignificant terms, simpler models were obtained which not only better explain the experimental data, but also are more powerful in predicting new conditions.

Now that the relationships have been developed, the test data were used to investigate the prediction ability of the models. Root mean square errors (RMSE) between calculated responses (C_i)

Table 4. Summary of the results from the statistical analysis of the models after eliminating the insignificant terms

	F	p-value	R^2	R^2_{adj}	R^2_{pred}
MFD	155.56	0.000	95.69%	95.08%	94.18%
StdFD	55.61	0.000	89.86%	88.25%	86.02%

and real responses (R_i) were determined using equation (11) for experimental data as well as test data for the sake of evaluation of both MFD and StdFD models and are listed in Table 5. Hence, the results imply the acceptable prediction ability of the models.

$$\text{RMSE} = \sqrt{\frac{\sum_{i=1}^{n}(C_i - R_i)^2}{n}} \tag{11}$$

Table 5 RMSE values of the models for the experimental and test data

	Experimental data	Test data
MFD	7.489	10.647
StdFD	2.493	2.890

Response surfaces for mean fiber diameter

Solution concentration

Increasing polymer concentration will result in greater polymer chain entanglements. This causes the viscoelastic force to increase enabling the charged jet to withstand a larger electrostatic stretching force leading to a larger diameter of fibers. A monotonous increase in MFD with concentration was observed in this study as shown in Fig. **4** (a), (b), and (c) which concurs with the previous observations [23], [29], [56]-[58]. The concentration effect was more pronounced at longer spinning distances (Fig. **4** (a)). This could be attributed to the twofold effect of distance which will later be discussed in the paper. At low concentrations, there are higher amounts of solvent in the solution and longer distance provides more time not only to stretch the jet in the electric field but also to evaporate the solvent, thereby favoring thinner fiber formation. At higher concentrations, however, there are extensive polymer chain entanglements resulting in higher viscoelastic forces which tend to resist the electrostatic stretching force.

Spinning distance

Increasing the spinning distance, the electric field strength will decrease ($E = \frac{V}{d}$) resulting in less acceleration, hence stretching of the jet which leads to thicker fiber formation. The balance between these two effects will determine the final fiber diameter. Increase in fiber diameter [57], [60], [61] as well as decrease in fiber diameter [29] with increasing spinning distance was reported in the literature. There were also some cases in which spinning distance did not have a significant influence on fiber diameter [56], [62]-[64]. The impact of spinning distance on MFD is illustrated in Fig. **4** (a), (d), and (e). As it is depicted in these figures, the effect of spinning distance is not always the same. Hence, the electrostatic stretching force, which has now become weaker, will be dominated easier by the viscoelastic force. As a result, the increasing effect of spinning distance on fiber diameter will be assisted, rendering higher MFD (Fig. **4** (a)). The effect of spinning distance will alter at different applied voltages (Fig. **4** (d)). The function of spinning distance was observed to be independent from the volume flow rate for MFD (Fig. **4** (e)). The interaction of spinning distance with solution concentration and applied voltage demonstrated in Fig. **4** (a) and (d), proved the existence of terms *Cd* and *dV* in the model of MFD.

Applied voltage

Increasing applied voltage may decrease [66]-[68], increase [56], [57], [61] or may not change [23], [29], [62], [69] the fiber diameter. Fig. **4** (b), (d), and (f) show the effect of applied voltage on MFD. Increasing the voltage, MFD underwent an increase followed by a decrease. The effect of voltage on MFD was influenced by solution concentration to some extent (Fig. **4** (b)). At high concentrations, the increase in fiber diameter with voltage was more pronounced. This could be attributed to the fact that the effect of the mass of solution will be more important for solutions of higher concentration. Spinning distance dramatically influenced the way voltage affects fiber diameter (Fig. **4** (d)). Looking at the figures, it is apparent that there is a huge interaction between applied voltage and spinning distance, a slight interaction between applied voltage and solution concentration and no interaction between applied voltage and volume flow rate which is in agreement with the presence of *CV* and *dV* and absence of *VQ* in the model of MFD.

Volume flow rate

It was suggested that a minimum value for solution flow rate is required to form the drop of polymer at the tip of the needle for the sake of maintaining a stable Taylor cone [70]. In this study, the MFD slightly increased with volume flow rate (Fig. **4** (c), (e), and (f)) which agrees with previous research [29], [70]-[72]. Flow rate was also found to influence MFD independent from solution

concentration, applied voltage, and spinning distance, as suggested earlier by the absence of *CQ*, *dQ*, and *VQ* in the model of MFD.

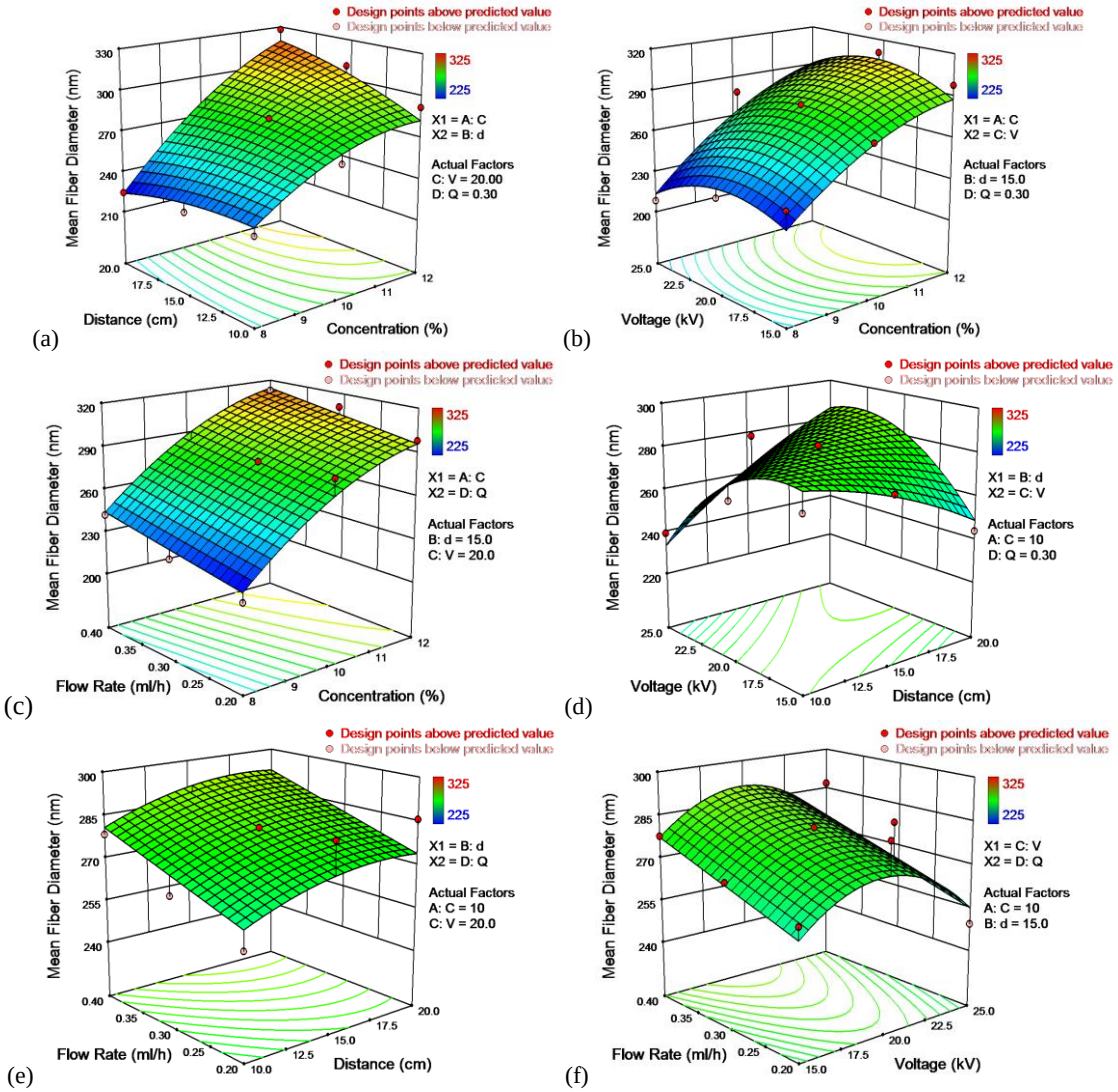

Fig. 4 Response surfaces for mean fiber diameter in terms of: (a) solution concentration and spinning distance, (b) solution concentration and applied voltage, (c) solution concentration and flow rate, (d) spinning distance and applied voltage, (e) spinning distance and flow rate, (f) applied voltage and flow rate

Response surfaces for standard deviation of fiber diameter

Solution concentration

As depicted in Fig. **5** (a), (b), and (c), StdFD increased with concentration which concurs with the previous observations [23], [31], [56], [59], [29], [61], [73], [74]. Concentration affected StdFD regardless of spinning distance (Fig. **5** (a)), suggesting that there was no interaction between these two parameters (absence of *Cd* in the model of StdFd). At low applied voltages, the formation of more uniform fibers upon decreasing the concentration was facilitated. In agreement with the existence of the term *CV* in the model of StdFd, solution concentration was found to have a slight interaction with applied voltage (Fig. **5** (b)). The curvature of the surface in Fig. **5** (c) suggested that there was a noticeable interaction between concentration and flow rate and this agrees with the presence of the term *CQ* in the model of StdFD.

Spinning distance

More uniform fibers (lower StdFD) were obtained on increasing the spinning distance as shown in Fig. **5** (a), (d), and (e). Our finding is consistent with the trend observed by Zhao *et al.* [74]. Spinning distance influenced StdFD regardless of solution concentration and applied voltage (Fig. **5** (a) and (d)) meaning that no interaction exists between these variables as could be inferred from the model of StdFD.

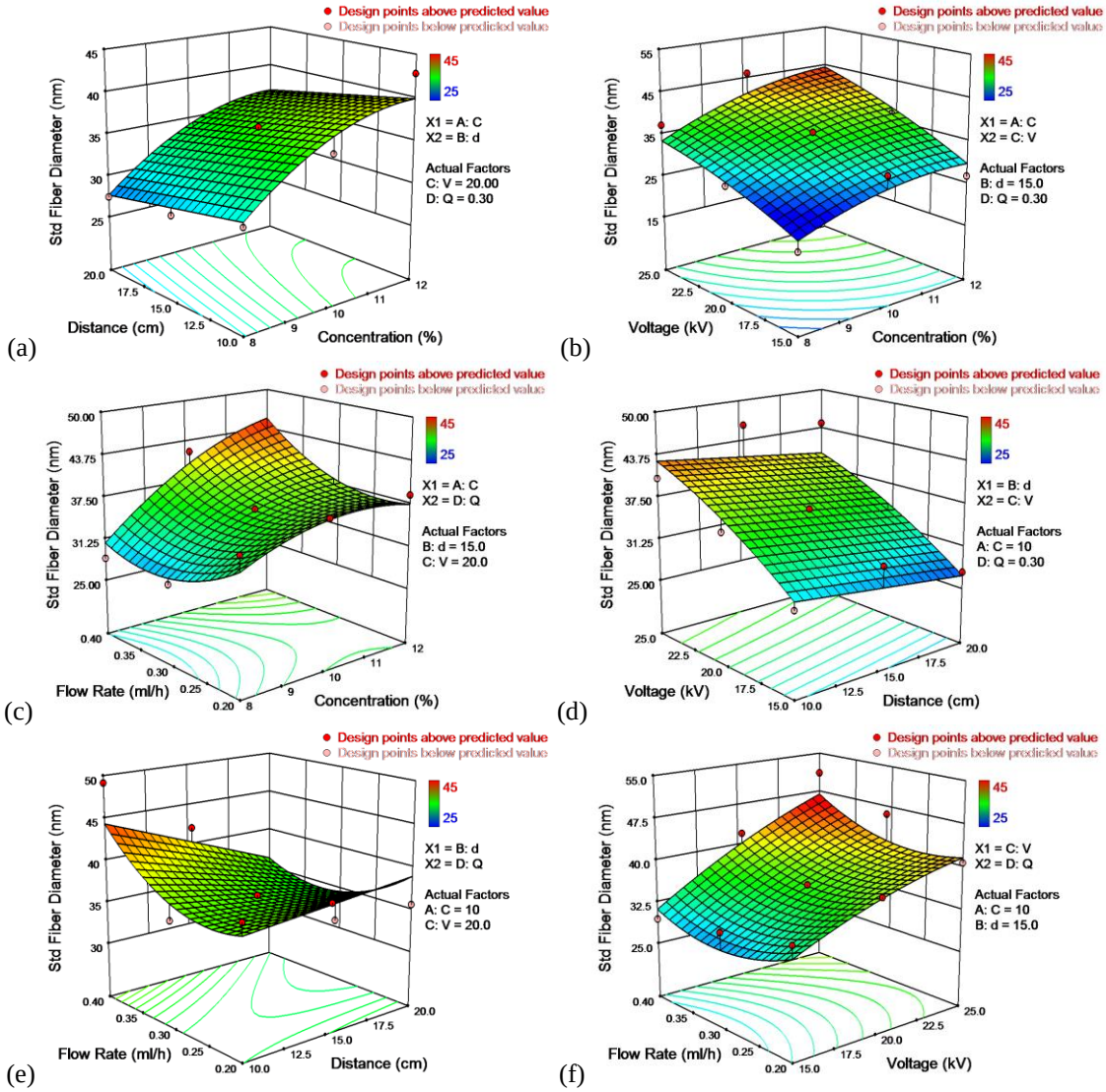

Fig. 5 Response surfaces for the standard deviation of fiber diameter in terms of: (a) solution concentration and spinning distance, (b) solution concentration and applied voltage, (c) solution concentration and flow rate, (d) spinning distance and applied voltage, (e) spinning distance and flow rate, (f) applied voltage and flow rate

Applied voltage

StdFD was found to increase with applied voltage (Fig. 5 (b), (d), and (f)), as observed in other works [56], [57], [61], [74]. The effect of applied voltage on StdFD was influenced by solution concentration as depicted in Fig. 5 (b), implying the interaction of voltage with concentration.

Volume flow rate

As demonstrated in Fig. **5** (c), (e), and (f), increasing the flow rate, the uniformity of fibers increased (StdFD decreased), reached an optimum value and then decreased (StdFD increased). When the flow rate is low, the amount of solution fed to the tip of the needle is not sufficient, whereas an excess amount of solution is delivered to the tip of the needle at high flow rates. The shorter the distance, the shorter is the time provided to the jet to thin and dry. Therefore, at high flow rates at which a larger amount of solution is delivered to the tip of the needle, the given time may not suffice, resulting in formation of less uniform fibers. High applied voltage favored the increase in StdFD at fast flow rates as depicted in Fig. **5** (f).

CONCLUSION

For MFD:

1- Increasing solution concentration, MFD increased rigorously. The effect of concentration was more pronounced at a longer spinning distance and at a higher applied voltage.

2- The effect of spinning distance on MFD changed depending on solution concentration and applied voltage. At low applied voltages, MFD decreased as the spinning distance became longer, whereas higher MFD resulted in lengthening the

spinning distance when the applied voltage was high. Increasing the solution concentration tended to assist the formation of thicker fibers at a longer spinning distance.

3- Rising the applied voltage, MFD was observed to first increase and then decrease. High solution concentrations partly and long spinning distances largely favored the increase of MFD with applied voltage.
4- MFD slightly increased with flow rate. The impact of flow rate on MFD was not related to the other variables.

For StdFD:

1- The higher the solution concentration, the less uniform fibers (higher StdFD) were formed. Low applied voltages facilitated the formation of more uniform fibers (lower StdFD) on decreasing the concentration. The increase of StdFD with concentration gained momentum at high flow rates.
2- Longer spinning distance resulted in more uniform fibers (lower StdFD). The effect of spinning distance was more pronounced at higher flow rates.
3- Rising the applied voltage increased StdFD. Low concentrations facilitated the formation of uniform fibers (high StdFD) with decreasing the applied voltage.
4- Flow rate was found to have a significant impact on the uniformity of fibers (StdFD). As the flow rate increased, StdFD decreased and then increased. Higher solution concentration, higher applied voltage, and shorter spinning distance favored the formation of non-uniform fibers (high StdFD) at fast flow rates.

REFERENCES

1. G.I. Taylor, *Proceedings of the Royal Society of London*, **313**, (1515), 453, (1969)
2. J. Doshi and D.H. Reneker, *Journal of Electrostatics*, **35**, 151, (1995)
3. H. Fong and D.H. Reneker, Electrospinning and Formation of Nanofibers, Chapter 6, 225-, In: D. R. Salem, Structure Formation in Polymeric Fibers, Hanser, Cincinnati, 2001.
4. D. Li and Y. Xia, *Advanced Mats*, **16**(14), 1151, (2004)
5. R. Derch, A. Greiner and J.H. Wendorff, Polymer Nanofibers Prepared by Electrospinning, In: J. A. Schwarz, C. I. Contescu and K. Putyera, Dekker Encyclopedia of Nanoscience and Nanotechnology, CRC, New York, 2004.
6. A.K. Haghi and M. Akbari, *Physica Status Solidi* (a), **204**, 1830, (2007)
7. P.W. Gibson, H.L. Schreuder-Gibson and D. Rivin, *AIChE Journal*, **45**,(1), 190, (1999)
8. Z.M. Huang, Y.Z. Zhang, M. Kotaki and S. Ramakrishna, *Composites Science and Technology*, **63**, 2223, (2003)
9. M. Li, M.J. Mondrinos, M.R. Gandhi, F.K. Ko, A.S. Weiss and P.I. Lelkes, *Biomats*, **26**, 5999, (2005)
10. E.D. Boland, B.D. Coleman, C.P. Barnes, D.G. Simpson, G.E. Wnek and G.L. Bowlin, *Acta Biomatia*, **1**, 115, (2005)
11. J. Lannutti, D. Reneker, T. Ma, D. Tomasko and D. Farson, *Mats Science and Engineering* C, **27**, 504, (2007)
12. J. Zeng, L. Yang, Q. Liang, X. Zhang, H. Guan, C. Xu, X. Chen and X. Jing, *Journal of Controlled Release*, **105**, 43, (2005)
13. E.R. Kenawy, G.L. Bowlin, K. Mansfield, J. Layman, D.G. Simpson, E.H. Sanders and G.E. Wnek, *Journal of Controlled Release*, **81**, 57, (2002)
14. M.-S. Khil, D.-I. Cha, H.-Y. Kim, I.-S. Kim and N. Bhattarai, *Journal of Biomedical Mats Research - Part B: Applied Biomats*, **67**, 675, (2003)
15. B.M. Min, G. Lee, S.H. Kim, Y.S. Nam, T.S. Lee and W.H. Park, *Biomats*, **25**, 1289, (2004)
16. X.H. Qin and S.Y. Wang, *Journal of Applied Polymer Science*, **102**, 1285, (2006)
17. J.S. Kim and D.H. Reneker, *Polymer Engineering and Science*, **39**,(5), 849, (1999)
18. S.W. Lee, S.W. Choi, S.M. Jo, B.D. Chin, D.Y. Kim and K.Y. Lee, *Journal of Power Sources*, **163**, 41, (2006)
19. C. Kim, *Journal of Power Sources*, **142**, 382, (2005)
20. N.J. Pinto, A.T. Johnson, A.G. MacDiarmid, C.H. Mueller, N. Theofylaktos, D.C. Robinson and F.A. Miranda, *Applied Physics Letters*, **83**,(20), 4244, (2003)
21. D. Aussawasathien, J.-H. Dong and L. Dai, , *Synthetic Metals*, **54**, 37, (2005)
22. S.-Y. Jang, V. Seshadri, M.-S. Khil, A. Kumar, M. Marquez, P.T. Mather and G.A. Sotzing, *Advanced Mats*, **17**, 2177, (2005)
23. S.-H. Tan, R. Inai, M. Kotaki and R. Ramakrishna, , *Polymer*, **46**, 6128, (2005)
24. A. Ziabicki, Fundamentals of Fiber Formation: The Science of Fiber Spinning and Drawing, Wiley, New York, 1976.
25. A. Podgóski, A. Bałazy and L. Gradoń, *Chemical Engineering Science*, **61**, 6804, (2006)
26. B. Ding, M. Yamazaki and S. Shiratori, *Sensors and Actuators* B, **106**, 477, (2005)
27. J.R. Kim, S.W. Choi, S.M. Jo, W.S. Lee and B.C. Kim, *Electrochimica Acta*, **50**, 69, (2004)
28. L. Moroni, R. Licht, J. de Boer, J.R. de Wijn and C.A. van Blitterswijk, *Biomats*, **27**, 4911, (2006)
29. T. Wang and S. Kumar, *Journal of Applied Polymer Science*, **102**, 1023, (2006)

30. S. Sukigara, M. Gandhi, J. Ayutsede, M. Micklus and F. Ko, *Polymer*, **45**, 3701, (2004)
31. S.Y. Gu, J. Ren and G.J. Vancso, *European Polymer Journal*, **41**, 2559, (2005)
32. S.Y. Gu and J. Ren, *Macromolecular Mats and Engineering*, **290**, 1097, (2005)
33. O.S. Yördem, M. Papila and Y.Z. Menceloğlu, *Mats and Design*, **29**, 34, (2008)
34. I. Sakurada, Polyvinyl Alcohol Fibers, CRC, New York, 1985.
35. F.L. Marten, Vinyl Alcohol Polymers, In: H. F. Mark, Encyclopedia of Polymer Science and Technology, 3rd Eddition, vol. 8, Wiley, 2004.
36. Y.D. Kwon, S. Kavesh and D.C. Prevorsek (Allied Corporation), Method of Preparing High Strength and Modulus Polyvinyl Alcohol Fibers, U. S. Patent, no. 4,440,711, April 3, 1984.
37. S. Kavesh and D.C. Prevorsek (Allied Corporation), Producing High Tenacity, High Modulus Crystalline Article Such as Fiber or Film, U. S. Patent, no. 4,551, 296, November 5, 1985.
38. H. Tanaka, M. Suzuki and F. Uedo (Toray Industries, Inc.), Ultra-High-Tenacity Polyvinyl Alcohol Fibers and Process for Producing Same, U. S. Patent, no. 4,603,083, July 29, 1986.
39. G. Paradossi, F. Cavalieri, E. Chiessim, C. Spagnoli and M.K. Cowman, *Journal of Mats Science: Mats in Medicine*, **14**, 687, (2003)
40. G. Zheng-Qiu, X. Jiu-Mei and Z. Xiang-Hong, *Bio-Medical Mats and Engineering*, **8**, 75, (1998)
41. M. Oka, K. Ushio, P. Kumar, K. Ikeuchi, S.H. Hyon, T. Nakamura and H. Fujita, *Journal of Engineering in Medicine*, **214**, 59, (2000)
42. K. Burczak, E. Gamian and A. Kochman, *Biomats*, **17**, 2351, 1996.
43. J.K. Li, N. Wang and X.S. Wu, *Journal of Controlled Release*, **56**, 117, (1998)
44. A.S. Hoffman, *Advanced Drug Delivery Reviews*, **43**, 3, (2002)
45. J. Zeng, A. Aigner, F. Czubayko, T. Kissel, J.H. Wendorff and A. Greiner, *Biomacromolecules*, **6**, 1484, (2005)
46. K.H. Hong, *Polymer Engineering and Science*, **47**, 43, (2007)
47. L.H. Sperling, Introduction to Physical Polymer Science, 4th Edition, Wiley, New Jersey, 2006.
48. J.C.J.F. Tacx, H.M. Schoffeleers, A.G.M. Brands and L. Teuwen, *Polymer*, **41**, 947, (2000)
49. F.K. Ko, Nanofiber Technology, Chapter 19, In: Y. Gogotsi, Nanomats Handbook, CRC Press, Boca Raton, 2006.
50. A. Koski, K. Yim and S. Shivkumar, *Mats Letters*, **58**, 493, (2004)
51. D.C. Montgomery, Design and Analysis of Experiments, 5th Edition, Wiley, New York, 1997.
52. A. Dean and D. Voss, Design and Analysis of Experiments, Springer, New York, 1999.
53. G.E.P. Box and N.R. Draper, Response Surfaces, Mixtures, and Ridge Analyses, Wiley, New Jersey, 2007.
54. K.M. Carley, N.Y. Kamneva and J. Reminga, Response Surface Methodology, CASOS Technical Report, CMU-ISRI-04-136, 2004.
55. S. Weisberg, Applied Linear Regression, 3rd Edition, Wiley, New Jersey, 2005.
56. C. Zhang, X. Yuan, L. Wu, Y. Han and J. Sheng, *European Polymer Journal*, **41**, 423, (2005)
57. Q. Li, Z. Jia, Y. Yang, L. Wang and Z. Guan, Preparation and Properties of Poly(Vinyl Alcohol) Nanofibers by Electrospinning, Proceedings of IEEE International Conference on Solid Dielectrics, Winchester, U. K., July 8-13, 2007.
58. C. Mit-uppatham, M. Nithitanakul and P. Supaphol, *Macromolecular Chemistry and Physics*, **205**, 2327, (2004)
59. Y.J. Ryu, H.Y. Kim, K.H. Lee, H.C. Park and D.R. Lee, *European Polymer Journal*, **39**, 1883, (2003)
60. T. Jarusuwannapoom, W. Hongrojjanawiwat, S. Jitjaicham, L. Wannatong, M. Nithitanakul, C. Pattamaprom, P. Koombhongse, R. Rangkupan and P. Supaphol, *European Polymer Journal*, **41**, 409, (2005)
61. S.C. Baker, N. Atkin, P.A. Gunning, N. Granville, K. Wilson, D. Wilson and J. Southgate, *Biomats*, **27**, 3136, (2006)
62. S. Sukigara, M. Gandhi, J. Ayutsede, M. Micklus and F. Ko, *Polymer*, **44**, 5721, (2003)
63. X. Yuan, Y. Zhang, C. Dong and J. Sheng, *Polymer International*, **53**, 1704, (2004)
64. C.S. Ki, D.H. Baek, K.D. Gang, K.H. Lee, I.C. Um and Y.H. Park, *Polymer*, **46**, 5094, (2005)
65. J.M. Deitzel, J. Kleinmeyer, D. Harris and N.C. Beck Tan, *Polymer*, **42**, 261, (2001)
66. C.J. Buchko, L.C. Chen, Y. Shen and D.C. Martin, *Polymer*, **40**, 7397, (1999)
67. J.S. Lee, K.H. Choi, H.D. Ghim, S.S. Kim, D.H. Chun, H.Y. Kim and W.S. Lyoo1, *Journal of Applied Polymer Science*, **93**, 1638, (2004)
68. S.F. Fennessey and R.J. Farris, *Polymer*, **45**, 4217, (2004)
69. S. Kidoaki, I. K. Kwon and T. Matsuda, *Biomats*, **26**, 37, (2005)
70. X. Zong, K. Kim, D. Fang, S. Ran, B.S. Hsiao and B. Chu, *Polymer*, **43**, 4403, (2002)
71. D. Li and Y. Xia, *Nano Letters*, **3**,(4), 555, (2003)
72. W.-Z. Jin, H.-W. Duan, Y.-J. Zhang and F.-F. Li, *Proceedings of the 1st IEEE International Conference on Nano/Micro Engineered and Molecular Systems*, 42, Zhuhai, China, January 18-21, 2006.
73. X.M. Mo, C.Y. Xu, M. Kotaki and S. Ramakrishna, *Biomats*, **25**, 1883, (2004)
74. S. Zhao, X. Wu, L. Wang and Y. Huang, *Journal of Applied Polymer Science*, **91**, 242, (2004)

СИСТЕМАТИЧНО ПАРАМЕТРИЧНО ИЗСЛЕДВАНЕ НА ПОЛУЧАВАНЕТО НА НАНОВЛАКНА ЧРЕЗ ЕЛЕКТРОПРЕДЕНЕ

М. Мохамадиан[1], А.К. Хаги[2*]

[1]*Департамент по текстилно инженерство, Ислямски университет „Азад“. клон Кашан, Иран*
[2]*Университет в Гилян, Ращ, Иран*

Получена на 16 юли, 2013 г.; коригирана на 29 август, 2013 г.

(Резюме)

Електропреденето е процес при който се получават непрекъснати полимерни влакна с суб-микронни диаметри. При електропреденето електричеката масова сила действа върху елемент от зареден флуид. Електропреденето е специализирана техника за образуването на суб-микронни влакна (с диаметри типично между 100 nm и 1 μm) с висока специфична повърхност. Целта на тази работа е да се установят количествени зависимости между параметрите на електропредене и средните и стандартните отклонения в диаметрите на влакната, както и да се оцени ефективността на намерените емпирични модели.